Point-contact spectroscopy of the nickel borocarbide superconductor YNi_2B_2C in the normal and superconducting state

D. L. Bashlakov, Yu. G. Naidyuk, I. K. Yanson
B. Verkin Institute for Low Temperature Physics and Engineering, National Academy of Sciences of Ukraine, 47 Lenin Ave., 61103, Kharkiv, Ukraine

G. Behr, S.-L. Drechsler, G. Fuchs, L. Schultz and D. Souptel
Leibniz-Institut für Festkörper- und Werkstoffforschung Dresden e.V., Postfach 270116, D-01171 Dresden, Germany
(Dated: February 6, 2008)

Point-contact (PC) spectroscopy measurements of YNi_2B_2C single crystals in the normal and superconducting (SC) state ($T_c \simeq 15.4$ K) for the main crystallographic directions are reported. The PC study reveals the electron-phonon interaction (EPI) spectral function with dominant phonon maximum around 12 meV and further weak structures (hump or kink) at higher energy at about 50 meV. No "soft" modes below 12 meV are resolved in the normal state. The PC EPI spectra are qualitatively similar for the different directions. Contrary, directional study of the SC gap results in $\Delta_{[100]} \approx 1.5$ meV for the a direction and $\Delta_{[001]} \approx 2.3$ meV along the c axis; however the critical temperature T_c in PC in all cases is near to that in the bulk sample. The value $2\Delta_{[001]}/k_BT_c \approx 3.6$ is close to the BCS value of 3.52, and the temperature dependence $\Delta_{[001]}(T)$ is BCS-like, while the for small gap $\Delta_{[100]}(T)$ is below BCS behavior at $T > T_c/2$ similarly as in the two-gap superconductor MgB_2. It is supposed that the directional variation Δ can be attributed to a multiband nature of the SC state in YNi_2B_2C.

PACS numbers: 72.10.Di, 74.45.+c, 74.70Dd

INTRODUCTION

The family of borocarbide superconductors RT_2B_2C, where R is a rare-earth element and T is a transition metal element (mainly Ni) have been studied intensively after superconductivity in RT_2B_2C was discovered in 1994 [1, 2]. Nevertheless, the nature and mechanism of superconductivity in borocarbides which have 3D electronic structure are still under debate. The most thermodynamic, transport and spectroscopic measurements [3, 4] give evidence that the superconducting (SC) state has an s-wave symmetry and the pairing is mediated by the electron-phonon interaction. However, for nonmagnetic R = Lu and Y compounds there are several properties mentioned in Ref.[5], which when taken together, might be interpreted also as hints for unconventional d-wave or p-wave superconductivity. An anisotropic s-wave order parameter (or s+g model) was proposed for $LuNi_2B_2C$ and YNi_2B_2C in [6]. Anyhow, irrespective of the actual order parameter symmetry, there is clear evidence for a notable anisotropy of the SC gap in YNi_2B_2C [7, 8, 9, 10, 11, 12, 13, 14] at least on parts of the complex Fermi surface [15, 16, 17].

Using point-contact (PC) spectroscopy [18] both the SC order parameter and the PC electron-phonon interaction (EPI) function $\alpha^2_{PC}F(\omega)$ can be determined from the first and second derivatives of the $I(V)$ characteristic of PC, respectively. The measurement of the second derivative of the $I(V)$ for PC provides straightforward information as to the PC EPI function $\alpha^2_{PC}F(\omega)$ [18, 19, 20]. The knowledge of $\alpha^2F(\omega)$ for conducting systems is a touchstone as to phonon-mediated superconductivity, which is governed by the value of the electron-phonon-coupling parameter $\lambda = 2\int \alpha^2F(\omega)\omega^{-1}d\omega$. Moreover, the comparison of the experimentally determined $\alpha^2F(\omega)$ with the calculated one can discriminate different theoretical models and approaches. Thus the PC spectroscopy could be helpful to illuminate details of the EPI in RT_2B_2C as well as to resolve non-phonon quasiparticle interactions. In addition, the SC gap determines the behavior of the $I(V)$ curve of PC at the low biases of a few mV, which is widely used to derive the SC gap from routine fitting by the well-known Blonder-Tinkham-Klapwijk (BTK) equations [21]. These experimental information as to the SC gap and EPI function is very useful for understanding the SC properties and the mechanism of superconductivity for the material under study.

Up to now there are a few papers where YNi_2B_2C has been investigated by PC spectroscopy [10, 11, 12, 22, 23, 24]. The first four papers are devoted to study of the SC gap, while the PC EPI spectra for YNi_2B_2C were measured and analyzed in [23, 24]. The main attention there was devoted to study the low energy part of the PC spectra and to so called "soft" mode at about 4-5 meV in the electron-quasiparticle spectrum. However, the measured PC spectra were featureless above 20 mV, although a number of pronounced phonon peaks are well resolved at higher energy by neutron spectroscopy [25]. In this paper we present more detailed data as to PC EPI spectra of YNi_2B_2C and as to directional measurements of the SC gap in this compound. The data were reported on M^{2}S-HTSC Conference in Dresden (July 9-14, 2006) and partially published in Physica C [26].

EXPERIMENTAL DETAILS

We have used single crystals of YNi_2B_2C grown by a floating zone technique with optical heating [27]. The sample has a residual resistivity of $\rho_0 \simeq 1\mu\Omega\,\mathrm{cm}$ and a residual resistivity ratio (RRR) about 40. It becomes superconducting at about 15.4 K with a transition width about 0.1 K. PCs were established both along the c axis and along the a axis as well as in the basal plane close to the [110] direction by standard "needle-anvil" or "shear" methods [18]. As a counter electrode Cu or Ag thin ($\oslash \simeq 0.15\,\mathrm{mm}$) wires were used to study the SC gap via the mechanism of Andreev reflection. A series of measurements were done using homocontacts between two pieces of YNi_2B_2C. In this case the orientation of the contact axis with respect to the crystallographic directions was not controlled. The experimental cell was placed in a flow cryostat, enabling measurements from 1.5 K up to T_c and higher. PCs were created by touching the YNi_2B_2C surface by sharpened Cu and Ag wires directly in the cryostat at liquid helium temperature. To establish homocontacts two pieces of YNi_2B_2C were touched. An disadvantage of the "needle–anvil" method is the sensitivity of the contacts to mechanical vibrations and to change of temperature. As a result, temperature measurements have sustained about a quarter from total in four tens of the contacts investigated at liquid helium temperature.

Using a technique of synchronous detection of weak alternating signal harmonics, the first harmonic of the modulating signal V_1 (proportional to the differential resistance $R(V) = dV/dI(V)$) and the second harmonic V_2 (proportional to $d^2V/dI^2(V)$) were recorded as a function of the bias voltage V. $V_2(V)$ can be expressed as follows:

$$V_2(V) = \frac{V_1^2}{2\sqrt{2}} R_0^{-1} \frac{dR(V)}{dV}. \qquad (1)$$

According to the theory of PC spectroscopy [19, 20] the second derivative $R^{-1}dR/dV = R^{-2}d^2V/dI^2(V)$ of the $I(V)$ curve of the ballistic contact at low temperatures is determined by the PC EPI function $\alpha^2_{\mathrm{PC}}F(\epsilon)$:

$$R^{-1}\frac{\mathrm{d}R}{\mathrm{d}V} = \frac{8\,\mathrm{e}d}{3\,\hbar v_{\mathrm{F}}} \alpha^2_{\mathrm{PC}}(\epsilon)\,F(\epsilon)|_{\epsilon=\mathrm{e}V}, \qquad (2)$$

where e is the electron charge, d is the PC diameter and α_{PC}, roughly speaking, reflects strength of the interaction of electrons with phonons. This interaction underlines the large-angle scattering (back-scattering) processes [19] of electrons in the PC constriction. Thus $\alpha^2_{\mathrm{PC}}F(\epsilon)$ is a kind of transport EPI function which selects phonons with a large momentum or Umklapp scattering. The PC diameter d, which enters in Eq.(2), can be calculated by the Wexler [28] relation:

$$R_{\mathrm{PC}}(T) \simeq \frac{16\rho l}{3\pi d^2} + \frac{\rho(T)}{d}, \qquad (3)$$

which consists of a sum of ballistic (Sharvin) and the diffusive (Maxwell) terms. Here $\rho l = p_{\mathrm{F}}/ne^2$ corresponds to the free electron model, where p_{F} is the Fermi momentum and n is the density of charge carriers. Using data for $\rho = 2.5\mu\Omega\,\mathrm{cm}$ and l=41 nm from [29] the product ρl is about $10^{-11}\Omega\,\mathrm{cm}^2$ in YNi_2B_2C.

From (1) and (2) $\alpha^2_{\mathrm{PC}}(\epsilon)\,F(\epsilon)$ can be defined as:

$$\alpha^2_{PC}(\epsilon)\,F(\epsilon) = \frac{3}{2\sqrt{2}} \frac{\hbar v_{\mathrm{F}}}{\mathrm{e}d} \frac{V_2}{V_1^2}, \qquad (4)$$

that is the measured ac voltage V_2 weighted by V_1^2 is directly proportional to the PC EPI function $\alpha^2_{\mathrm{PC}}(\epsilon)\,F(\epsilon)$. Here it is necessary to mention that the finite temperature T and the alternating voltage V_1 result in a smearing of the measured V_2 spectra. Thus, the infinitely narrow spectral peak smears into a bell-shaped maximum (see, e. g. [18]) with the width

$$\delta = [(5.44\,\mathrm{k_B}T/\mathrm{e})^2 + (1.22\sqrt{2}\,V_1)^2]^{1/2}. \qquad (5)$$

For example, the smearing of a PC spectrum measured at liquid helium temperature 4.2 K and at ac voltage V_1 between 1 and 2 mV, mainly used in our measurements, is between 2.6 and 4 mV.

The PC EPI function $\alpha^2_{PC}(\epsilon)\,F(\epsilon)$ should vanish above the maximum phonon energy $\hbar\omega_{\max}$, which is close to the Debye energy $k_{\mathrm{B}}T_{\mathrm{D}}$, because of the lack of phonons with larger energy. Therefore, according to (4) the PC spectrum $V_2(V)$ should vanish above $eV \geq \hbar\omega_{\max}$. In fact, measured PC spectra always have a nonzero almost constant value above the Debye energy, the so-called background. The general nature of the background was understood by taking into account an accumulation of nonequilibrium phonons in the PC region created by the energized electrons. The details of the background calculations are given elsewhere [20, 30]. The most often semiempirical formula [18]

$$B(eV) = \mathrm{const} \int_0^{eV} \frac{\alpha^2_{\mathrm{PC}}(\epsilon)F(\epsilon)}{\epsilon}\mathrm{d}\epsilon \qquad (6)$$

is used to describe the background. Here for calculations of the energy dependent background an iterative procedure is applied taking as a first approximation for $B(eV)$ a curve, which continuously increases from zero to the maximal background value at $eV \geq \hbar\omega_{\max}$.

In the case of a heterocontact between two metals the PC spectrum represents a sum of the contributions from both metals 1 and 2 weighted by the inverse Fermi velocity [31]:

$$\frac{V_2}{V_1^2} \propto \upsilon \frac{(\alpha^2F)_1}{v_{F1}} + (1-\upsilon)\frac{(\alpha^2F)_2}{v_{F2}}, \qquad (7)$$

where υ is the relative volume occupied by metal 1 in the PC. Thus, using of heterocontacts enables also, e. g., qualitative estimation of the relative strength of EPI in

the investigated material as compared to some standard or well known one.

According to the BTK theory [21] of conductivity of N-c-S heterocontacts (here N is the normal metal, c is the constriction and S is the superconductor) a maximum at zero-bias voltage and a double-minimum structure at about $V \simeq \pm\Delta/\mathrm{e}$ in the $\mathrm{d}V/\mathrm{d}I$ curves manifest the Andreev reflection processes at the N-S interface with a finite, so called, barrier strength parameter $Z \neq 0$. The latter has a simple interpretation: it increases normal state resistance of the PC by a factor of $(1+Z^2)$. Thus, as it was mentioned, the minima position in $\mathrm{d}V/\mathrm{d}I$ reflect roughly the SC gap value, which follows from the equations for the $I(V)$ characteristics [21]:

$$I(V) \sim \int_{-\infty}^{\infty} T(\epsilon)\,(f(\epsilon - \mathrm{e}V) - f(\epsilon))\,\mathrm{d}\epsilon, \qquad (8)$$

$$T(\epsilon) = \frac{2\Delta^2}{\epsilon^2 + (\Delta^2 - \epsilon^2)(2Z^2+1)^2}, \quad |\epsilon| < \Delta$$

$$T(\epsilon) = \frac{2|\epsilon|}{|\epsilon| + \sqrt{\epsilon^2 - \Delta^2}(2Z^2+1)}, \quad |\epsilon| > \Delta\ ,$$

where f(ϵ) is the Fermi distribution function. In general, Z characterizes reflection (or transmission) of the N-S interface, which is defined also by the mismatch of the Fermi velocity v_F. Thus, even in the absence of a "natural" barrier Z is non zero and is given by

$$Z = \frac{|v_{F_1} - v_{F_2}|}{2(v_{F_1} v_{F_2})^{1/2}}\ . \qquad (9)$$

The smearing of the experimental dV/dI curves as compared to the calculated ones according to (8) is usually attributed to quasiparticle DOS N(ϵ, Γ) broadening in the superconductor due to finite-lifetime. According to Dynes et al. [32] it can be taken into account by adding an imaginary part to the energy ϵ, namely, ϵ is replaced by $\epsilon - i\Gamma$ in (8). We used (8) to fit the measured $\mathrm{d}V/\mathrm{d}I$ curves of PCs and to extract the SC gap.

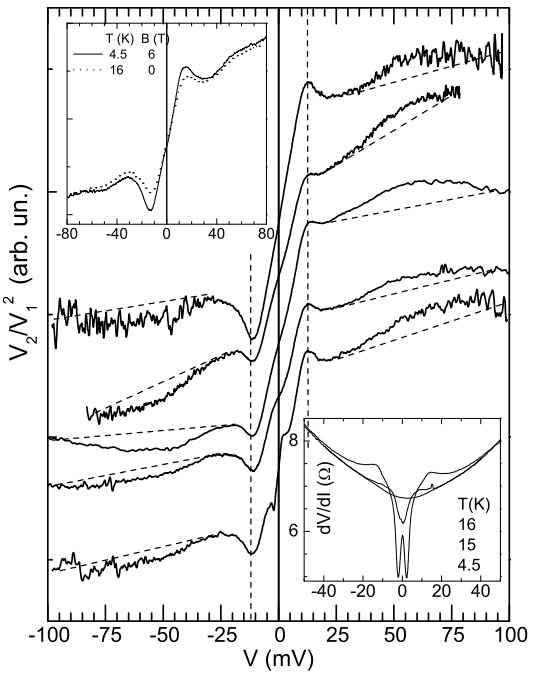

Figure 1: PC spectra [see Eq. (4)] of several YNi_2B_2C–Ag contacts with resistance 8.8, 6.8, 3.1, 2.8 and 5.1Ω (from the top curve to the bottom one). PC spectra are measured at 16 K $>T_c \simeq$15.4 K to suppress superconductivity and avoid huge features in V_2 between $\sim \pm$20 mV due to the gap minimum shown in the bottom inset. The bottom curve (measured at 15.1 K – slightly below T_c) demonstrates these almost suppressed (sharp kink/peak) features close to zero bias. Vertical dashed lines are drawn to help to follow position of the main maximum in the PC spectra and tilted lines are drawn to accentuate hump around 50 mV. Upper inset shows PC spectra of YNi_2B_2C–Cu contacts with resistance 4.5 Ω measured at $V_1(0)$=2 mV in the normal state by suppressing superconductivity via temperature or magnetic field.

EXPERIMENTAL RESULTS AND DISCUSSION

PC spectroscopy of quasiparticle excitations

Figure 1 shows PC spectra of several YNi_2B_2C–Ag heterocontacts for which the SC gap has been measured simultaneously. We have selected the PC spectra for which the SC gap varies (see Fig. 4) gradually from the maximal value of 2.5 meV (upper spectrum) to the minimal one of 1.65 meV (bottom spectrum). However, no qualitative difference between PC EPI spectra is observed. The spectra show a dominant maximum at about 12 mV and a broad shallow maximum or hump centered around 50 mV (Fig. 1). These maxima correspond well to the phonon DOS maxima at 12 and 50 mV of YNi_2B_2C (see Fig. 2) obtained by neutron diffraction [25]. At the same time the PC spectra do not contain contributions from the other phonon maxima at 20, 24, 32 mV and 100 mV observed in the phonon DOS. In this context we should mention that PC spectra of $HoNi_2B_2C$ [33] display mentioned phonon maxima near 20, 24, 32 mV. Contrary, the PC spectra of YNi_2B_2C above 12 mV is monotonic and almost featureless, except of the mentioned 50 mV feature. Of course, the increase of noise with the voltage hides details of the spectra at higher energies. Note also, that the spectra in Fig. 1 are measured in the normal state at 16 K where the resolution due to the Fermi level smearing is according to (5) about 8 meV which can mask fine features. However, as the upper insert in Fig. 1 shows, the spectrum measured at 4.5 K (solid curve) with the resolution of about 4 meV is similar to the other one

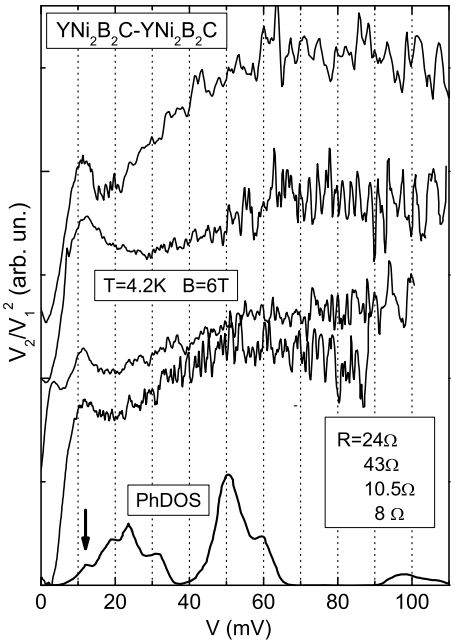

Figure 2: PC spectra [see Eq. (4)] of several YNi_2B_2C–YNi_2B_2C homo contacts with different resistance (shown in inset). The PC spectra are measured in magnetic field 6 T to suppress SC features at low bias. The PC spectrum for 10.5 Ω contact still shows maximum around 4 mV due to residual superconductivity. The bottom curve shows phonon density of states (PhDOS) for YNi_2B_2C from [25].

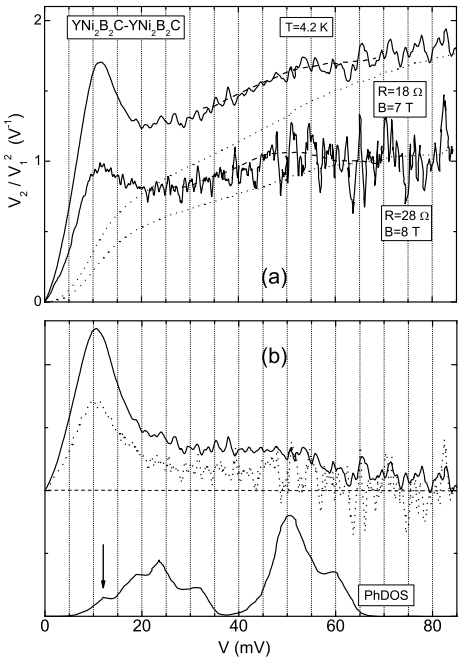

Figure 3: (a) PC spectra [see Eq. (4)] of two YNi_2B_2C homocontacts averaged for two polarities. The superconductivity is suppressed by a magnetic field. Dotted curves show the background behavior calculated according to (6). Dashed curves on the PC spectra are drawn by hand to better visualize hump around 50 mV. $V_1(0)$ is 0.7 and 0.87 mV, which gives δ=2.3 and 2.5 mV according to (5). (b) PC spectra from the upper panel after subtracting of the background. The bottom curve shows PhDOS for YNi_2B_2C [25]. Vertical arrow shows position of the maximum in PhDOS which corresponds to the main maximum in the PC spectra.

(dashed curve) only it has a little bit sharper maximum at 12 mV. Even improving resolution below 3 mV (see Fig. 3) does not recover additional details of the spectra. It means that the instrumental broadening of the spectra does not play here a crucial role. In this respect we should note that according to recent data [34] the strong EPI gives rise to pronounced anomalies in the phonon dispersion curves of YNi_2B_2C and concurrently to *large line widths* of certain phonon modes. The latter along with selection of the large-angle scattering processes in PC can be responsible for the broad and less detailed (compared to PhDOS) structure in PC EPI spectra.

By interpreting the PC spectra of heterocontacts we have to take into account for possible contributions of the normal metal (e.g., Ag or Cu) used as a counter electrode. To avoid this we have measured PC spectra of homocontacts shown in Fig. 2. No qualitative difference in the spectra of homo and heterocontacts is seen (compare spectra in Figs. 1 and 2). Thus, the contribution of Ag or Cu in the presented PC spectra of heterocontacts (see, Fig. 1) is negligible. Apparently, low Fermi velocities in nickel borocarbides [3, 4] as compared to the noble metals accentuate the contribution of YNi_2B_2C in the PC spectra according to Eq. (7).

Fig. 3 displays the PC spectra of two homocontacts averaged for negative and positive polarity. Here also the behavior of the background obtained from (6) and the neutron phonon DOS are shown. According to neutron data [25] there is a gap around 40 meV, which separates acoustic and optic phonon branches. In this energy region only a flattering occurs in our PC spectra after subtracting of the background. The main reason is that subtraction of the background for PC spectra with a high background level is not a straightforward procedure. Nevertheless, the PC spectra show two remarkable features – a maximum at about 12 mV and a hump around 50 mV. Similar PC EPI spectra of YNi_2B_2C were presented in [23, 24]. Here we only note that the measured *normal* state PC EPI spectra of YNi_2B_2C demonstrate no "soft" modes around 4–5 mV discussed by Yanson et al. [23, 24] and noticed by Martinez-Samper et al. [9] in STM spectra. Similar to "soft" mode maxima are seen in the bottom spectrum in Fig. 1 and in the spectrum of

10.5 Ω-contact in Fig. 2, but they can be attributed to superconductivity which is not fully suppressed in these contacts.

After subtracting the background from the measured PC spectra the EPI function is established according to Eq.(4) (see Fig. 3b) and the EPI parameter $\lambda = 2\int \alpha^2 F(\omega)\omega^{-1}d\omega$ is calculated, which is found to be about 0.1. However, the calculation of λ from a PC spectrum is complicated for several reasons. First of all equation (4) is derived for a free electron model and a single band Fermi surface. Secondly, deviations from the ballistic regime in PC due to elastic scattering have to be corrected by a pre-factor l_i/d in (4), where l_i is the elastic electron mean free path and d is the PC diameter. However, l_i is difficult to evaluate for the PC. In this case only a qualitative estimation of λ is possible taking into account that contribution of Ag or Cu in the PC spectra of YNi_2B_2C–Ag/Cu heterocontacts in Fig. 1 (PC spectra of YNi_2B_2C–Cu heterocontact is shown in inset) is hardly to resolve. From the latter we can conclude that the intensity of the EPI function in YNi_2B_2C is at least larger than that in Cu, where $\lambda \simeq 0.25$ [18]. This provides an complementary confirmation of the moderate EPI in YNi_2B_2C with the lower limit of 0.25 for the λ [41]. Note also that because the 12 mV-maximum prevails in the PC spectra, the main (about 90%) contribution to λ_{PC} comes from the energy region below 35 meV corresponding to the low energy (acoustic) part of the phonon DOS. Calculation of EPI coupling in YNi_2B_2C revealed that about 70% of λ results from the nine lowest branches [34].

No significant anisotropy of the PC EPI spectra in YNi_2B_2C was observed (see, e.g., Fig. 1). The main reason can be that the spectra are quite broad and smeared, what hides the fine structure of EPI, which might be anisotropic. However, isotropic behavior of the resistivity in YNi_2B_2C mentioned in [3, 4] is in line with almost isotropic PC spectra.

Directional PCS of the SC energy gap

As it was mentioned above the SC gap manifests itself in the dV/dI characteristic of a N-c-S contact as minima around $V \simeq \pm\Delta$ if $Z \neq 0$ and a temperature is well below T_c. Such dV/dI curves are presented in Fig. 4 for several contacts whose PC spectra are shown in Fig. 1. dV/dI in Fig. 4 reflects also the distribution of the gap in YNi_2B_2C.

The gap distribution is also shown in Fig. 5 for a cleaved nonoriented rough YNi_2B_2C surface. The characteristic values of the fitting parameters are shown in Table I. The distribution in Fig. 5 is similar to that observed for YNi_2B_2C films [12]. Different from the films is that the gap values in Fig. 5 stretched above 2.4 meV. Note, that the average gap is close to the BCS value of $\Delta = 1.76 k_B T_c \simeq 2.3$ meV. Interesting that using effective

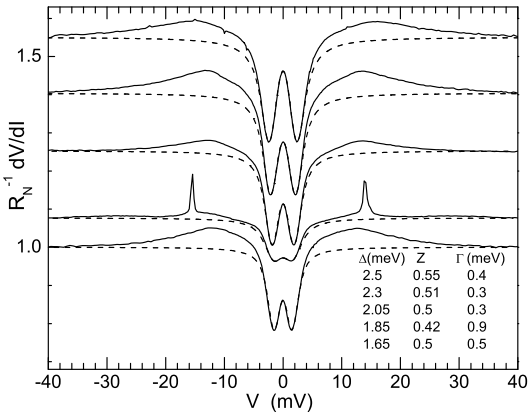

Figure 4: Reduced dV/dI curves (solid lines) of YNi_2B_2C–Cu contacts at T=4.2 K. PC spectra for these contacts are shown in Fig. 1. Dashed lines are BTK fitting curves according to (8). The curves are shifted vertically versus the bottom one for clarity. The table shows SC energy gap Δ, Γ and Z parameters obtained by BTK fitting of the experimental curves.

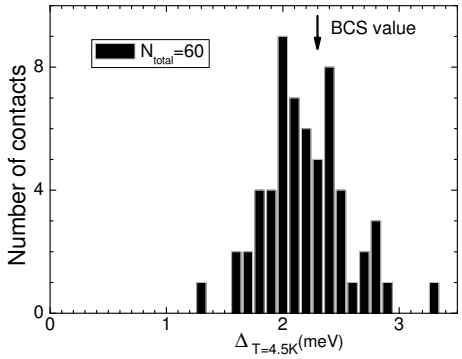

Figure 5: Gap distribution measured for a cleaved nonoriented surface of YNi_2B_2C single crystal.

Fermi velocities in YNi_2B_2C in the range from 0.45×10^5 to 4.5×10^5 m/s [17] within the two-band model [29] and a typical Fermi velocity of Cu 1.57×10^6 m/s, the barrier parameter Z can be estimated according to (9) to be between 0.67 and 2.9 values, that is the lower value is close to the maximal Z from the Table I.

Table I: Average, minimal and maximal values of the SC gap Δ, 'smearing' parameter Γ and 'barrier' parameter Z for PCs represented gap distribution in Fig. 5.

	Δ(meV)	Γ(meV)	Z
Average	**2.2**	**0.64**	**0.5**
Minimal	1.3	0.3	0.33
Maximal	3.3	2.3	0.69

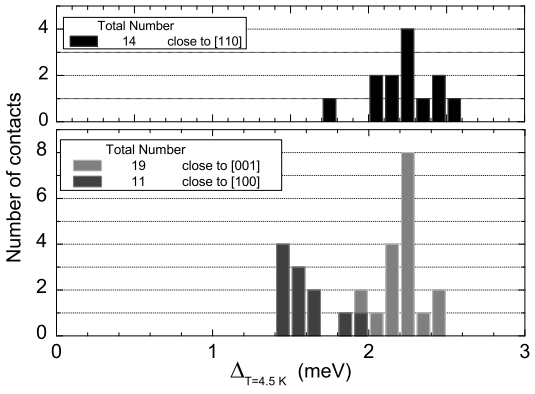

Figure 6: Gap distribution for the three main directions in YNi_2B_2C single crystal. In comparison with our gap distribution presented in [26], here, the data are added measured for 21 contact for YNi_2B_2C with improved RRR $\simeq$ 60. But it makes no qualitative changes, only improves statistic.

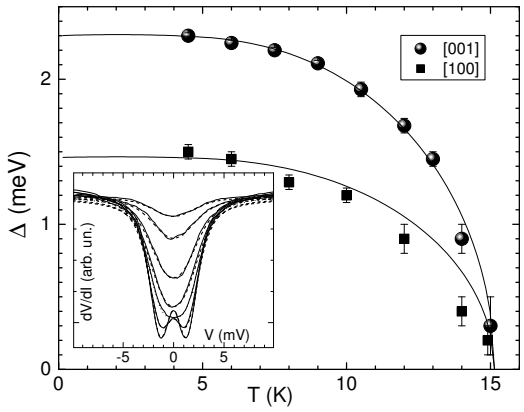

Figure 8: Temperature dependence of the small (1.5 meV) and large (2.3 meV) gap in YNi_2B_2C. Solid curves represent BCS-like behavior. Inset shows normalized to the normal state dV/dI curves (solid) for the small gap along with calculated curves (dashed) according to (8).

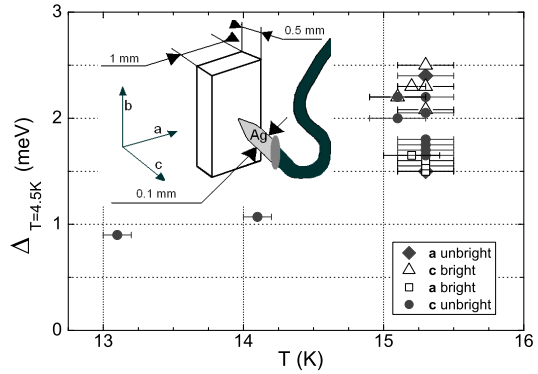

Figure 7: Gap distribution for the polished (bright) and unpolished (unbright) surface of YNi_2B_2C single crystal for two main directions versus critical temperature in PC. Inset shows draft of the YNi_2B_2C single crystal and sharpened Ag wire.

The gap distribution for different crystallographic orientations in YNi_2B_2C is shown in Fig. 6. The anisotropy in the distribution is clearly seen: a small gap is characteristic for the a-axis, while along the c-axis the gap is larger. Also the [110] direction has in average a slightly enhanced gap.

To exclude the gap variation due to surface degradation we have checked also the critical temperature of the gap vanishing for most of PCs. In Fig. 7 gap values for the a and c axis for the surface before polishing (marked by dark symbols) and after mechanical polishing and chemical etching (marked by bright symbols) are plotted against the critical temperature T_c of the PC. It is seen that for two PCs with low gap value of about 1 meV T_c is reduced as compared to the bulk one, therefore, a degradation of the SC state at the surface is likely responsible for the low gap value ($\leq$ 1 meV) rather than an anisotropy of the gap. Contrary, different gap values for PCs with the same T_c shown in Fig. 7 gives unequivocal evidence of intrinsic reason of the gap variation.

It is noted that the derived gap values are fairly consistent with recent specific heat data [14]. Here it was shown that the two-gap model with Δ=2.67 meV and 1.19 meV describe the SC gap function of YNi_2B_2C better than other models based on the isotropic s-wave, the d-wave line nodes, or the s+g wave approach. Furthermore, as it was shown in [35] two-gap fit better describes $dV/dI(V)$ curve of PCs in the sister compound $LuNi_2B_2C$.

The temperature dependence of Δ for two PCs with different gaps is shown in Fig. 8. It is seen that $\Delta(T)$ has in general BCS-type dependence. The gap is found to vanish close to the bulk T_c. However, the small gap deviates from the BCS curve by approaching T_c. Similar (small) gap behavior is characteristic for the well-known multiband (two-gap) superconductor MgB_2 [36]. Thus the mentioned observations of the gap behavior and distribution can be taken as support of two-gap scenario in YNi_2B_2C. At the same time as follows from recent ARPES experiments [13], the momentum-dependent superconducting gap shows a large anisotropy ($\Delta = 2.3 - 3.2$ meV) observed on a single FS. Also ultrahigh-resolution photoemission spectra [37] are better described by anisotropic s-wave gap in the form $\Delta(\theta) = 2.8|\cos 2\theta|$ (meV). Therefore, the gap behavior in YNi_2B_2C is rather complex, showing both anisotropic and multiband superconductivity.

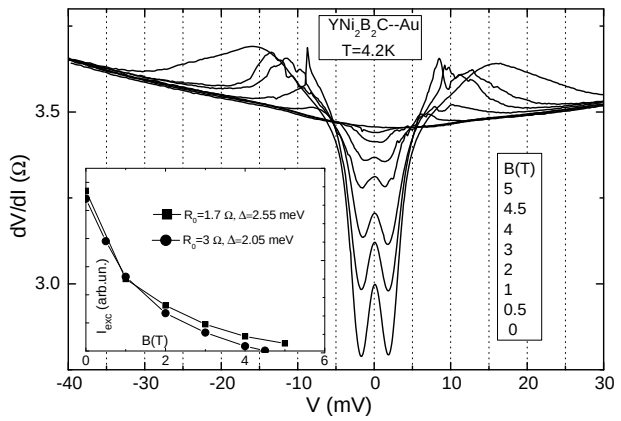

Figure 9: Magnetic field dependence of dV/dI curves for YNi_2B_2C–Au contact. Inset shows behavior of the excess current for this contact and for another one with larger Δ.

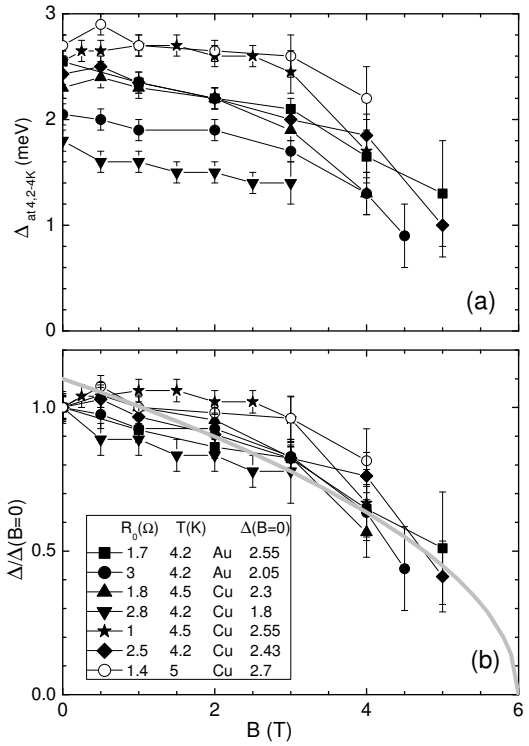

Figure 10: Magnetic field dependence of the SC gap at 4.2 K in YNi_2B_2C extracted from dV/dI for a few contacts: (a) SC gap in absolute value, (b) SC gap reduced to $\Delta(B = 0)$. Grey curve shows the behavior $\propto (1 - B/B_{c2})^{1/2}$ of the pair potential of a type II superconductor in the vortex state according to Abrikosov's theory.

Magnetic field behavior of the SC energy gap and excess current

In Fig. 9 the field dependence of dV/dI curves for a YNi_2B_2C–Au contact is shown. A remarkable suppression of the minimum in dV/dI is observed for applied field above 3 T. This increases of the error in the determination of the Δ value and makes calculations of Δ less accurate, especially close to the critical field. The latter can be estimated of about 6 T from the SC features (minimum) disappearing in dV/dI, that is it is close to the bulk critical field at helium temperature 4.5 K (see e. g. [29]). $\Delta(B)$ behavior extracted from the dV/dI curves for this and several other contacts is shown in Fig. 10. In general, $\Delta(B)$ exhibits a conventional behavior decreasing with overall negative curvature. At the same time the excess current $I_{\rm exc}$, which is roughly speaking proportional to the area of the gap minimum in dV/dI (or more precisely to the area of the gap maximum in differential conductivity dI/dV), decreases with the magnetic field with a positive curvature (see Fig. 9 inset). Similar $I_{\rm exc}(B)$ behavior we have recently reported for PC on YNi_2B_2C film [12] and before a remarkable positive curvature in $I_{\rm exc}(B)$ has been observed for the two-band superconductor MgB_2 [38]. As it was shown for the first time in [39], the excess current of an S-c-N contact is governed by Δ or SC order parameter [40]. Indeed, the temperature dependence of $I_{\rm exc}(T)$ (not shown) is similar to the $\Delta(T)$ dependence, that is $I_{\rm exc}(T)$ has a negative curvature, while $I_{\rm exc}(B)$ does not. In [38] the model was proposed that in the mixed state of type-II superconductor $I_{\rm exc}$ is proportional not only to $\Delta(B)$, but also to the SC volume, outside vortices. The size of the contacts in Fig. 10 can be estimated from (3) in a few tens of nanometers, while coherence length in YNi_2B_2C is about 5–8 nm [3, 4]. Therefore a number of vortices can penetrate the PC area at a field approaching B_{c2}.

CONCLUSION

We have carried out investigations of the electron-phonon spectral function and the SC energy gap in YNi_2B_2C by PCS. We have measured PC EPI spectra of YNi_2B_2C in the normal state showing the dominant phonon maximum at about 12 meV along with hump or kink around 50 meV. Position of these features in the PC spectra corresponds to the maxima in the phonon DOS measured by neutron diffraction. However most of the phonon peaks are not resolved in the PC spectra. The reason can be weak contribution of some phonons into large-angle electron-phonon scattering in PC and/or large line widths of certain phonon modes. We did not found appreciable difference in the PC EPI spectra for PCs demonstrating different SC gap value, what may testify that the gap variation (anisotropy) is connected with

the electronic structure.

The observed variation of the gap is such that the small gap ($\Delta \sim$1.5 meV) is characteristic for the direction along the a-axis, while along the c-axis the gap is higher ($\Delta \sim$2.3 meV) and similar or slightly larger gap is measured for the [110] direction. The directional variation Δ along with the absence of marked anisotropy of PC EPI spectra can be an issue of complex multiband ground state in YNi_2B_2C. Multiband scenario for the SC state is also supported by the observation of the small gap and the excess current behavior for YNi_2B_2C similar as in the two-gap(band) superconductor MgB_2.

Acknowledgements

The support of the *Deutsche Forschungsgemeinschaft* within SFB 463 "Rare earth transition metal compounds: structure, magnetism and transport", the U.S. Civilian Research and Development Foundation for the Independent States of the Former Soviet Union (grant no. UP1-2566-KH-03) and of the National Academy of Sciences of Ukraine are acknowledged. The investigations were carried out in part with the help of donated by A. von Humboldt Foundation (Germany) equipments.

[1] R. J. Cava, H. Takagi, H. W. Zandbergen, J. J. Krajewski, W. F. Peck Jr., T. Siegrist, B. Batlogg, R. B. van Dover, R. J. Felder, K. Mizuhashi, J. O. Lee, H. Eisaki, S. Uchida, Nature **367** 252 (1994).

[2] R. Nagarajan, C. Mazumdar, Z. Hossain, S. K. Dhar, K. V. Gopalakrisnan, L. C. Gupta, C. Godart, B. D. Padalia, R. Vijayaraghavan, Phys. Rev. Lett. **72** (1994) 274.

[3] K.-H. Müller, V. N. Narozhnyi, Rep. Prog. Phys. **64**, 943 (2001).

[4] K.-H. Müller, G. Fuchs, S.-L. Drechsler and V. N. Narozhnyi, in: *Magnetic and Superconducting Properties of Rare Earth Borocarbides of the Type RNi_2B_2C*, Handbook of Magnetic Materials, (Ed. K. H. J. Buschow), Elsevier North-Holland, Vol. 14, (2002), pp. 199-305.

[5] S.-L. Drechsler, S. V. Shulga, K.-H. Müller, G. Fuchs, J. Freudenberger, G. Behr, H. Eschrig, L. Schultz, M. S. Golden, H. von Lips, J. Fink, V. N. Narozhnyi, H. Rosner, P. Zahn, A. Gladun, D. Lipp, A. Kreyssig, M. Loewenhaupt, K. Koepernik, K. Winzer, K. Krug, Physica C **317-318**, 117 (1999).

[6] K. Maki, P. Thalmeier, and H. Won, Phys. Rev. B **65**, 140502 (2002).

[7] K. Izawa, K. Kamata, Y. Nakajima, Y. Matsuda, T. Watanabe, M. Nohara, H. Takagi, P. Thalmeier, K. Maki, Phys. Rev. Lett. **89**, 137006 (2002).

[8] T. Park, E. E. M. Chia, M. B. Salamon, E. D. Bauer, I. Vekhter, J. D. Thompson, E. M. Choi, H. J. Kim, S.-I. Lee, P. C. Canfield, Phys. Rev. Lett. **92**, 237002 (2004).

[9] P. Martinez-Samper, H. Suderow, S. Vieira, J. P. Brison, N. Luchier, P. Lejay, and P. C. Canfield, Phys. Rev. B 67, 014526 (2003).

[10] P. Raychaudhuri, D. Jaiswal-Nagar, Goutam Sheet, S. Ramakrishnan, and H. Takeya, Phys. Rev. Lett. **93**, 156802 (2004).

[11] S. Mukhopadhyay, Goutam Sheet, P. Raychaudhuri, H. Takeya, Phys. Rev. B **72**, 014545 (2005).

[12] D. L. Bashlakov, Yu. G. Naidyuk, I. K. Yanson, S. C. Wimbush, B. Holzapfel, G. Fuchs and S-L Drechsler, Supercond. Sci. Technol. **18**, 1094 (2005).

[13] T. Yokoya, T. Baba, S. Tsuda, T. Kiss, A. Chainani, S. Shin, T. Watanabe, M. Nohara, T. Hanaguri, H. Takagi, Y. Takano, H. Kito, J. Itoh, H. Harima, T. Oguchi, J. of Physics and Chemistry of Solids **67**, 277 (2006).

[14] C. L. Huang, J.-Y. Lin, C. P. Sun, T. K. Lee, J. D. Kim, E. M. Choi, S. I. Lee, and H. D. Yang, Phys. Rev. B **73**, 012502 (2006).

[15] S.-L. Drechsler, H. Rosner, I. Opahle, and H. Eschrig, Physica C **408**, 104 (2004).

[16] S.-L. Drechsler, I. Opahle, S. V. Shulga, H. Eschrig, G. Fuchs, K.-H. Müller, W. Löser, H. Bitterlich, G. Behr, and H. Rosner, Physica B **329**, 1352 (2003).

[17] S.-L. Drechsler, H. Rosner, S. V. Shulga, I. Opahle, H. Eschrig, J. Freudenberger, G. Fuchs, K. Nenkov, K.-H. Müller, H. Bitterlich, W. Löser, G. Behr, D. Lipp, and A. Gladun, Physica C **364-365** 31 (2001).

[18] Yu. G. Naidyuk and I.K. Yanson, *Point-Contact Spectroscopy*, Springer Series in Solid-State Sciences, Vol.145 (Springer Science+Business Media, Inc, 2005).

[19] I. O. Kulik, A. N. Omelyanchouk, R. I. Shekhter, Fiz. Nizk. Temp. **3**, 1543 (1977) [Sov. J. Low Temp. Phys. **3**, 840 (1977)].

[20] I. O. Kulik, Fiz. Nizk. Temp. **18**, 450 (1992) [Sov. J. Low Temp. Phys. **18**, 302 (1992)].

[21] G. E. Blonder, M. Tinkham, T. M. Klapwijk, Phys. Rev. B **25**, 4515 (1982).

[22] L. F. Rybaltchenko, I. K. Yanson, A. G. M. Jansen, P. Mandal, P. Wyder, C. V. Tomy, D. McK Paul, Physica B **218**, 189 (1996).

[23] I. K. Yanson, V. V. Fisun, A. G. M. Jansen, P. Wyder, P. C. Canfield, B. K. Cho, C. V. Tomy and D. McK Paul, Phys. Rev. Lett. **78** 935 (1997).

[24] I. K. Yanson, V. V. Fisun, A. G. M. Jansen, P. Wyder, P. C. Canfield, B. K. Cho, C. V. Tomy, D. M. Paul, Fiz. Nizk. Temp. **23**, 951 (1997) [Low Temp. Phys. **23**, 712 (1997)].

[25] F. Gompf, W. Reichardt, H. Schober, B. Renker, M. Buchgeister, Phys. Rev. B **55**, 9058 (1997).

[26] Yu. G. Naidyuk, D. L. Bashlakov, I. K. Yanson, G. Fuchs, G. Behr, D. Souptel, and S.-L. Drechsler, to be published in Physica C (2007).

[27] D. Souptel, G. Behr, W. Löser, K. Nenkov, G. Fuchs, J. of Crystal Growth, **275**, e91 (2005).

[28] A. Wexler, Proc. Phys. Soc. (London) **89**, 927 (1966).

[29] S. V. Shulga, S.-L. Drechsler, G. Fuchs, K.-H. Müller, K. Winzer, M. Heinecke, and K. Krug, Phys. Rev. Lett. **80**, 1730–1733 (1998).

[30] I. O. Kulik, Fiz. Nizk. Temp. **11**, 937 (1985) [Sov. J. Low Temp. Phys. **11**, 516 (1985)].

[31] R. I. Shekhter and I. O. Kulik, Fiz. Nizk. Temp. **9**, 46 (1983) [Sov. J. Low Temp. Phys. **9**, 22 (1983)].

[32] R. C. Dynes, V. Naraynamurti, J. P. Garno, Phys. Rev. Lett. **41**, 1509 (1978).

[33] Yu. G. Naidyuk, O. E. Kvitnitskaya, I. K. Yanson, G. Fuchs, K. Nenkov, S.-L. Drechsler, G. Behr, D. Souptel, K. Gloos, Physica B **359-361**, 469 (2005).

[34] W. Reichardt, R. Heid, and K. P. Bohnen, J. of Superconductivity, **18**, 759 (2005).

[35] N. L. Bobrov, S. I. Beloborod'ko, L. V. Tyutrina, V. N. Chernobay, I. K. Yanson, D. G. Naugle and K. D. D. Rathnayaka, Fiz. Nizk. Temp. **32**, 641 (2006) [Low Temp. Phys. **32**, 489 (2006)].

[36] P. Szabó, P. Samuely, J. Kačmarčik, T. Klein, J. Marcus, D. Fruchart, S. Miraglia, C. Marcenat, and A. G. M. Jansen, Phys. Rev. Lett. **87**, 137005 (2001).

[37] T. Baba, T. Yokoya, S. Tsuda, T. Kiss, T. Shimojima, S. Shina, T. Togashi, C. T. Chen, C. Q. Zhang, S. Watanabe, T. Watanabea, M. Nohara, H. Takagi, Physica B **378-380**, 469 (2006).

[38] Yu. G. Naidyuk, O. E. Kvitnitskaya, I. K. Yanson, S. Lee, and S. Tajima, Solid State Commun. **133**, 363 (2005).

[39] S. N. Artemenko, A. F. Volkov and A. V. Zaitsev, Solid State Communs. **30**, 771 (1979).

[40] S. I. Beloborod'ko, A. N. Omelyanchouk, Fiz. Nizk. Temp. **17**, 994 (1991) [Sov. J. Low Temp. Phys. **17**, 518 (1991)].

[41] By discussion of the λ value calculated from PC spectra we should always to bear in mind that λ_{PC} is some kind of transport λ and it can be, in general, different from the thermodynamic one. Moreover, as we have discussed in the case of $HoNi_2B_2C$ compound (Yu. G. Naidyuk et al., will be published) different bands can have different λ, while from PC spectra some average λ_{PC} is calculated.